EFDA–JET–PR(04)05

X. Garbet, P. Mantica, F. Ryter, G. Cordey, F. Imbeaux, C. Sozzi, E. Asp,
V.Parail, R. Wolf and JET EFDA contributors

Profile Stiffness and Global Confinement

Profile Stiffness and Global Confinement

X. Garbet[1], P. Mantica[2], F. Ryter[3], G. Cordey[4], F. Imbeaux[1], C. Sozzi[2], E. Asp[1], V.Parail[4], R. Wolf[5] and JET EFDA contributors*

[1]*Association EURATOM -CEA, CEA Cadarache, 13108 St Paul-Lez-Durance, France.*
[2]*Istituto di Fisica del Plasma CNR-EURATOM, via Cozzi 53, 20125 Milano, Italy.*
[3]*MPI für Plasmaphysik, EURATOM-Assoziation, D-8046 Garching bei München, Germany*
[4]*EURATOM/UKAEA Fusion Association, Culham Science Centre, Abingdon, OX14 3DB, UK*
[5]*Institut für Plasmaphysik, Association EURATOM / FZJ, D-52425 Jülich, Germany*
** See annex of J. Pamela et al, "Overview of Recent JET Results and Future Perspectives",
Fusion Energy 2000 (Proc. 18th Int. Conf. Sorrento, 2000), IAEA, Vienna (2001).*

ABSTRACT.

This paper analyses the properties of a critical gradient transport model based on a few assumptions: electrostatic gyroBohm scaling law, existence of an instability threshold, and finite background transport below the threshold. This model is characterised by only 3 scalar parameters. A quantitative criterion of stiffness is proposed, which provides a mean for a quantitative assessment and inter-machine comparison. It is also shown that this transport model is compatible with a two term scaling law of global confinement, as proposed recently by the ITPA-CDBM Group (International Tokamak Physics Activity - Confinement Data Base and Modelling Topical Group). This model has also been applied to analyse a variety of experiments using mostly electron heat modulation on JET, ASDEX-Upgrade and FTU. The thresholds are found to be in the expected domain for micro-instabilities in tokamaks. The stiffness factor is found to cover a broad range of variation. One possible cause is the ratio of electron to ion temperature, which is found to exhibit a correlation with the stiffness factor.

1. INTRODUCTION

The question of profile stiffness in tokamak plasmas has been debated for years [1,2,3,4,5,6,7]. Up to know, and in spite of a wealth of results, this debate did not lead to a clear conclusion. This suggests that some conditions have to be fulfilled to observe stiff profiles. Also a new element was introduced in the discussion, which comes from a recent result of the Confinement Data Base and Modelling (CDBM) Topical Group in the frame of the International Tokamak Physics Activity (ITPA). It was found that the confinement time is fairly well described by a two term scaling law that separates the contributions of the bulk and pedestal in H-mode plasmas [8]. These two contributions exhibit different parametric dependences, whereas an assumption of strong stiffness would lead to similar scaling laws.

Part of the contradiction comes from some ambiguity in the definition of stiffness. Stiff profiles are commonly defined as marginally stable profiles, i.e. profiles whose gradients are very close to the instability threshold everywhere. However, a less stringent characterisation is to define a number χ_S, the stiffness factor, which quantifies the ratio between the diffusivity and the difference between the temperature gradient and its critical value κ_c, with an appropriate normalisation. Strong stiffness corresponds to a large value of χ_S. It is also often forgotten that the diffusivity stays finite below the instability threshold. This property is obviously true for ions since the diffusivity cannot be lower than the neoclassical value, which is not negligible. The neoclassical diffusivity of electrons is very small. However it is plausible that a finite turbulent diffusivity exists below the threshold, for instance due to some residual small scale turbulence or to turbulence propagation. Assuming an electrostatic gyroBohm scaling law, one is led to a transport model that is characterised by 3 numbers: a threshold κ_c, a stiffness factor χ_S and a background diffusivity χ_0.

There exist already many transport models that involve an instability threshold. One may quote RLW [9], Weiland [10], IFS-PPPL [11], GLF23 [12], Multi-Mode (MMM) [13] and OHE [14]

models. The concept of diffusivity with two contributions, a large and a small one, also underlies the mixed Bohm-gyroBohm model [15]. Stiffness is usually assessed by predicting profiles using one or several models and comparing them with measurements. This has been done extensively during the recent years [4,7,16,17]. Another strategy was proposed recently [18,19,20]. It consists in identifying the reduced set of parameters that characterise the simplified transport model described above. This identification was made possible by analysing experiments where the heating source is modulated. Both steady and modulated profiles provide some information in this case. In particular, the threshold can be determined with accuracy by using the change of slope that is observed on the radial profiles of amplitude and phase of modulated temperature. The drawback is obviously that this simplified model does not cover all the physics known from first principle turbulence simulations. However, it offers many advantages. First, an interpretative analysis can be done in an efficient way, i.e. the parameters of this model can be directly identified from experimental results, and compared in different plasma conditions or machines. Second, this transport model has analytical (or semi-analytical) solutions so that some exact results can be obtained and tested. In particular, quantitative conditions for getting stiff profiles can be derived. Finally, it provides an easy access to the scaling law of global confinement. The latter property is used here to clarify the compatibility with a two-term global scaling law.

The paper is organised as follows. The transport model is described in section II. Conditions for stiffness are given in section III, while the global confinement time is assessed in section IV. Finally a comparison with experimental results based on existing modulation experiments and on the ITPA-CDBM two-term scaling law is done in section V. A summary and conclusion follow.

2. A MINIMAL TRANSPORT MODEL

The aim of this section is to derive a simple transport model that preserves some basic properties of turbulent transport. The main hypothesis is a turbulent transport characterised by an electrostatic gyroBohm scaling law, switched on above a threshold $-R\partial_r T/T = \kappa_c$ [21]. Here r is a label of flux surface with a dimension of length. The assumption of gyroBohm scaling relies on several recent turbulence simulations in the limit of small values of ρ^* [22,23,24,25]. However, one has to bear in mind that a substantial departure from gyroBohm scaling is found when the diamagnetic E×B velocity shear rate is large [22,24] or when turbulence spreading takes place [25]. Below the threshold, the diffusivity is finite and is produced by collisions for ions, or by some background of turbulence for electrons. To simplify the calculation, the scaling law of this background diffusivity is supposed to be also gyroBohm (this means that the dependence on temperature is wrong when the background diffusivity is neoclassical). With these assumptions, the thermal diffusivity is of the form

$$\chi_T = \chi_s q^\nu \frac{T}{eB} \frac{\rho_S}{R} \left(\frac{-R\partial_r T}{T} - \kappa_c \right) H \left(\frac{-R\partial_r T}{T} - \kappa_c \right) + \chi_0 q^\nu \frac{T}{eB} \frac{\rho_S}{R} \tag{1}$$

where is the Larmor radius, $\rho s = \sqrt{m_i T}/eB$ is a number that characterises the stiffness, and H(x) is

2

a Heaviside function. The safety factor has been introduced to account for the improvement of confinement with plasma current. It is also consistent with profiles of diffusivity that increase radially. The exponent ν is adjusted once for all when comparing various devices. The value $\nu = 3/2$ was chosen in the present work, as it seems to be the best compromise, and allows to recover the scaling of the two term scaling law with plasma current (see section V). Recent simulations of Ion Temperature Gradient (ITG) driven turbulence provide some justification of this choice [26], since the parameter n was found to range between 1 and 2. Still this choice cannot be considered as definitive. Once the parameter†n is chosen, this transport model is characterised by 3 dimensionless constants χ_0, χ_s, κ_c, to be determined from experiments. These parameters may depend on plasma parameters such as the ratio of electron to ion temperature Te/Ti, the effective charge number Zeff, the density gradient length, and/or the ratio of the magnetic shear to the safety factor s/q depending on the underlying instability. The present analysis is valid if the 3 parameters χ_0, χ_s, κ_c are radially uniform for a given plasma. Thus χ_0, χ_s, κ_c may differ from one set of experiments to another one. Still the assumption that χ_0, χ_s, κ_c are uniform is a limitation. For instance the threshold is known to vary radially in Tore Supra [3].

For each species, the steady-state temperature is a solution of the heat equation, the heat flux being determined by the Fourier law

$$\Gamma_T = -n\chi_T \partial_r T \tag{2}$$

Using the transport model Eq.(1), it can be rewritten as (see appendix A)

$$\tau'\left(\frac{\tau'}{\tau} - 1\right)H\left(\frac{\tau'}{\tau} - 1\right) + \lambda_0\tau' = g \tag{3}$$

τ is a normalised temperature

$$\tau = \left(\frac{T}{T_{gB}}\right)^{5/2} \tag{4}$$

and is a function of the normalised spatial coordinate

$$\rho = \frac{5}{2}\kappa_c\frac{a - r}{R} \tag{5}$$

A prime indicates a derivative with respect to ρ. The parameter

$$\lambda_0 = \frac{\chi_0}{\kappa_c\chi_s} \tag{6}$$

characterises the relative degree of stiffness and is supposed to be smaller than 1. The function $g(\rho)$ is a heat flux normalised to the edge value (see appendix A). The temperature T_{gB} is determined by the relation

$$\Gamma_T(a) = \chi_s \kappa_c{}^2 q_a{}^\nu n_a T_{gB} \frac{T_{gB}}{eB} \frac{\rho_{s,gB}}{R^2} \tag{7}$$

where the flux $\Gamma_T(a)$ is the heat flux at the edge, q_a the edge safety factor, n_a the edge density and $\rho_{s,gB} = \sqrt{m_i T_{gB}}/eB$ is the Larmor radius calculated with the temperature T_{gB}. The temperature T_{gB} plays a central role in this work. It exhibits the usual "gyroBohm" scaling and may be recast in a more convenient way when the geometry is elliptical (see appendix A)

$$T_{eB,\,keV} = 1.89 \left(\frac{1+\kappa^2}{2\kappa}\right)^{-2/5} \chi_s{}^{-2/5} \kappa_c{}^{-4/5} M^{-1/5} \varepsilon_a{}^{-2/5} q_a{}^{-2\nu/5} B_T{}^{4/5} n_{a,19}{}^{-2/5} P_{MW}{}^{2/5} \tag{8}$$

Since each species may be characterised by a different set of parameters χ_0, χ_s, and κ_c, the temperature T_{gB} can be different for electron and ions. In the expression (8), P_{MW} is the additional power for one species.

The equation (3) can be rephrased in the following way:

i) above the threshold, $\tau' > \tau$, the temperature gradient is solution of the equation

$$\tau'^2 - \tau(1-\lambda_0)\tau' - g\tau = 0 \tag{9}$$

or equivalently

$$\tau' = \frac{(1-\lambda_0)\tau}{2} + \left[\frac{(1-\lambda_0)^2\tau^2}{4} + g\tau\right]^{1/2} \tag{10}$$

ii) below the threshold, $\tau' > \tau$, the temperature gradient is solution of the equation

$$\tau' = \frac{g}{\lambda_0} \tag{11}$$

In the case where the normalised heat flux is a radially uniform or an exponential, the solution of the heat equation (3) is analytical (see Appendix B). In the general case, the first order Eqs.(10) and (11) are easily solved numerically. The paper will be illustrated with the choice $\lambda_0 = 0.025$ and a normalised flux g of the form

$$g = \frac{a}{r} \exp\left[-x_s^2\left\{\left(\frac{a}{r}\right)^2 - 1\right\}\right] \tag{12}$$

The parameter xs characterises the heat source localisation and is chosen as $x_s = 0.3$ throughout this paper. The boundary condition is an edge temperature $T = Ta$ at $r = a$. For an H mode, Ta is the height of the pedestal.

3. CONDITIONS FOR STIFFNESS.

The analysis of equations (10) and (11) shows that the plasma can be divided in three regions:

1) an edge region where the temperature is low and the gradient is well above the threshold. This region exists when T<<TgB (i.e. τ<<1). An approximate solution of Eq.(11) is

$$\tau = \left(\tau_a^{1/2} + \frac{1}{2} \int_0^\rho d\rho g(\rho) \right)^2 \tag{13}$$

2) a stiff region where the temperature is high τ>>1, and the gradient is above the threshold. An approximate solution when λ_0<<1 is the well known exponential shape

$$\tau \approx C e^\rho \tag{14}$$

Using the heat flux conservation $\Gamma_T = -n_0 \chi_T \partial_r T$, it is found that for a stiff profile $\partial_r T = -n_0 \kappa_c T$, the heat diffusivity is given by $\chi_T = \Gamma_T/(n_0 \kappa_c T)$. Thus the heat diffusivity decreases when the temperature increases along the radial profile. This behaviour may appear paradoxical at first sight. It results from a temperature that increases faster than its gradient, as shown by Eq.(10) (see also Fig.1). Hence the temperature gradient length gets closer to the threshold when approaching the magnetic axis. The transition between the edge and stiff regions is smooth. It is decided arbitrarily here that the boundary $\rho = \rho_{gB}$ between the two regions corresponds to $\tau = 1$. For a constant heat flux, the logarithmic derivative of the temperature $-\partial_r T/\kappa_c T$ is a unique function of the temperature T/T_{gB}, as indicated by Eq.(10). For a given class of heat profiles, all these curves are close to each other (see Fig.1).

3) a region where the temperature is high and its logarithmic derivative is below the threshold. In the following, we will refer to this non-stiff region as the "core region". The solution of Eq.(11) is

$$\tau = \frac{1}{\lambda_0} \int_0^\rho d\rho g(\rho)$$

The transition between the stiff and core regions is sharp and occurs at the position where $\tau = \tau' = g/\lambda_0$. This equation defines a position $\rho = \rho_{cr}$ and a critical temperature $T_{cr} = g(\rho_{cr})T_{gB}/\lambda_0$. Explicit expressions of ρ_{cr} and ρ_{gB} are given in Appendix B. The transition temperature depends essentially on the reference temperature T_{gB} and the stiffness factor λ_0. It also depends on the normalised heat flux $g(\rho)$: when the deposition profile is flatter, the stiff region is thinner. A localised deposition profile leads to a flux g that behaves as a/r, thus moving the location of the transition towards the axis. This transition corresponds to the point where turbulence vanishes (note however that a turbulence may propagate from unstable to stable regions). The hot core is therefore a quiescent region (or weakly turbulent depending on the meaning of χ_0).

In summary the temperature profile is stiff in a layer $\rho_{cr}<r<r_{gB}$, where r_{gB} is the radius such that $\tau = 1$, and $r_{cr}/a = 1-\rho_{cr}/\rho_{max}$, where ρ_{cr} is defined above. An example is shown in figure 2. Figure 3 gives the dependence of these radii on the edge temperature for $\lambda_0 = 0.025$.

At this point, three main conclusions may be drawn:

i)   the edge region disappears when increasing the edge temperature, i.e. when $T_a \gg T_{gB}$. This condition expresses that the edge is stiff when the pedestal is high enough (it comes from the $T^{3/2}$ dependence of the diffusivity). We note that T_{gB} does not depend on the machine size (see Eq. (8)). So the difference of stiffness observed in various devices has to be explained with other considerations. When increasing T_a/T_{gB}, the hot core region broadens, thus reducing the width of the stiff region. For instance when $T_a = 2T_{gB}$ and $\lambda_0 = 0.025$, the stiff region only covers a half of the plasma.

ii) Stiffness is controlled by the stiffness factor χ_s. However the extension of the core region depends on the relative degree of stiffness $\lambda_0 = \chi_0/(\kappa_c \chi_s)$. In particular there is no core region if $\kappa_0 = 0$, whatever χ_s. The transition temperature between the stiff and core regions behaves as $1/\lambda_0$. For instance, for $\lambda_0 = 0.001$, the temperature profile is stiff almost everywhere. An example is shown in figure 4.

iii) a scan on the source radial width indicates that the stiff region is wider when the heat source is more centrally localised (i.e. when decreasing the parameter x_s). This comes from the fact that at a given radius close to the axis, the heat flux increases thus maintaining $-\nabla_r T/T$ more easily above the threshold. The non stiff core region is thus reduced.

In summary the condition for the plasma to be stiff everywhere is twofold $\tau_a \gg 1$ and $\lambda_0 \ll 1$, or equivalently $T_a \gg T_{gB}$ and $\chi_0 \ll \kappa_c \chi_s$. Peaked deposition profiles enhance the stiffness.

4. TWO TERM SCALING LAW AND STIFF TRANSPORT MODEL.

Once the heat equation has been solved for each species, the energy content and confinement time can be calculated. Some simplification is necessary to allow a comparison to a scaling law of global confinement time. It is assumed here that the model of diffusivity Eq.(1) is the same for electrons and ions, with the same threshold κ_c, degree of stiffness λ_0 and normalised heat flux g, but possibly different stiffness factors χ_{se} and χ_{si} (and therefore different background diffusivities to maintain λ_0 constant). Also the density, and the ratio of electron to ion temperatures are supposed to be radially constant. Adding the electron and ion heat equations eliminates the equipartition term. The resulting heat equation is the same as before (i.e. Eqs(1) and (2)) except that κ_s is now an effective stiffness factor. Solving in the average temperature $T = (T_e + T_i)/2$, this effective stiffness factor appears to be

$$\chi_{s,\,eff} = \frac{\chi_{s,\,i} + \left(\dfrac{T_e}{T_i}\right)^{5/2}\chi_{s,\,e}}{\left[0.5\left(1 + \dfrac{T_e}{T_i}\right)\right]^{5/2}} \qquad (15)$$

The confinement time is then of the form

$$\tau_E \approx C_\tau \tau_{gB} \qquad (16a)$$

6

where

$$C_\tau = \frac{1}{\rho_{max}} \int_0^{\rho_{max}} d\rho J \tau^{2/5} \qquad (16b)$$

and τ_{gB} is given in the Appendix A, Eq.(A11). The function J is $J = nV'/naV'a$. We limit the calculation to the case of an elliptical geometry so that $J = 2r/a = 2(1 - \rho/\rho_{max})$. It is stressed that P_{MW} is now the total additional power. The temperature profile and the form factor C_τ, are parameterised by the normalised edge temperature T_a/T_{gB}, the stiffness λ_0, and the heat source localisation x_s. This confinement time includes the energy content associated to the pedestal. Thus it differs from the "core confinement time" defined by the Confinement Database ITPA group [8]. To avoid any confusion we will call the latter confinement time of the plasma bulk. Hence the plasma bulk covers the 3 regions (core, stiff and edge) previously defined. The edge temperature T_a is the height of the pedestal. Following the prescription of the ITPA group, the confinement time of the plasma bulk is defined as

$$\tau_{Ebulk} \approx C_{ITPA} \tau_{gB} \qquad (17)$$

The form factor is now given by the relation

$$C_{ITPA} = C_\tau - \frac{T_a}{T_{gB}} = \frac{1}{\rho_{max}} \int_0^{\rho_{max}} d\rho J (\tau^{2/5} - \tau_a^{2/5}) \qquad (18)$$

The transport model Eq.(1) predicts a global confinement time of the form

$$\tau_{Ebulk} = 01.79 C_{ITPA} \chi_{s,eff}^{-2/5} \kappa_C^{-4/5} C^{-1/5} \kappa_C^{7/5} \left(\frac{1 + \kappa^2}{2} \right)^{-2/5} \qquad \epsilon_a^{8/5} R^3 B^{4/5} q_a^{-2v/5} n_{a,19}^{3/5} P_{MW}^{-3/5} \qquad (19)$$

with the same conventions as the ITPA group. Since the ITPA database is dominated by plasmas with equal ion and electron temperatures, the effective stiffness parameter is $\chi_{s,eff} = \chi_{s,e} + \chi_{s,i}$.

This scaling law is compatible with the ITPA result if the form factor C_{ITPA} depends weakly on the edge temperature. This is obviously not true in general. It is therefore interesting to analyse the dependence of C_{ITPA} on the edge temperature. Using the solution found above, the form factor C_τ is decomposed in the following manner

$$C_\tau = C_{\tau edge} + C_{\tau stiff} + C_{\tau core} \qquad (20)$$

$$C_{\tau edge} = \frac{1}{\rho_{max}} \int_0^{\rho_{gB}} d\rho J \tau^{2/5} ; \quad C_{\tau stiff} = \frac{1}{\rho_{max}} \int_{\rho_{gB}}^{\rho_{cr}} d\rho J \tau^{2/5} ; \quad C_{\tau core} = \frac{1}{\rho_{max}} \int_{\rho_{cr}}^{\rho_{max}} d\rho J \tau^{2/5} \qquad (21)$$

If the temperature profile is stiff everywhere, i.e. if $\tau_a \gg 1$ and $\lambda_0 \ll 1$, then $C_{\tau edge} = 0$,

$$C_{\tau core} = 0 \text{ and } C_{\tau stiff} = 2 \left(\frac{1}{2\rho_{max}} \right)^2 \left\{ e^{\frac{2\rho_{max}}{5}} - \frac{2\rho_{max}}{5} - 1 \right\} \frac{T_a}{T_{gB}} \tag{22}$$

With the present choice of parameters, this expression reduces to . Therefore the form factor of a stiff profile is proportional to the edge temperature, as expected. The global confinement time is then essentially determined by the pedestal height. An extreme case $\lambda_0 = 0.001$ is shown in figure 5. For a stiff profile the core confinement is not gyroBohm unless the edge temperature T_a follows a gyroBohm scaling law. This is not usually the case. Therefore a stiff profile is incompatible with the result found by the ITPA group.

At this point, a legitimate question is whether a non stiff transport model fulfils a two term separation criterion. The answer is negative. This can be understood by using the present transport model in another extreme situation where there is no stiff nor edge region ($r_{cr} = a, \tau_{cr} = \tau_a$). A simple calculation shows that the form factor varies with the edge temperature as

$$C_{\tau ITPA,core} \approx \frac{\rho_{max}}{2\lambda_0} \left(\frac{T_a}{T_{gB}} \right)^{-3/2} \tag{23}$$

This result can be tested by building an artificial case $\lambda_0 = 0.9$ for which the temperature is not stiff for $T_a > T_{gB}$. As expected from Eq.(23), it is found that C_{ITPA} decreases strongly with the edge temperature (see figure 5). Hence it does not satisfy the condition for a separation between pedestal and bulk. More generally, the separation between pedestal and bulk is rigorous for a diffusion coefficient that depends on the temperature gradient only (i.e. $\chi_T \propto \nabla T^{\alpha}$). For instance, a unique electrostatic gyroBohm model, $\chi_T \propto \nabla T^{3/2}$, satisfies this requirement.

In the general case, the form factor is the sum of edge, stiff and core contributions. As mentioned before, the core contribution increases with the edge temperature whereas the edge contribution decreases. The contribution of the stiff region is non monotonic. It follows the width of the stiff region. From Fig.3, one expects a bell shape. The detailed dependence of these form factors is difficult to assess in general, but can be easily determined numerically. Some asymptotic results are given in the Appendix C. A "typical" case $\lambda_0 = 0.025$ is shown on figure 6. It turns out that the trade-off between the edge, stiff and core regions leads to a form factor (as defined by the ITPA-CDBM group) that is less sensitive to the edge temperature than in the non stiff or very stiff cases (see the comparison on Fig.5). This behaviour occurs in spite of a profile that is stiff over a significant part of the plasma.

5. COMPARISON WITH EXPERIMENT
5.1 PARAMETERS OF THE TRANSPORT MODEL

Several groups have used previously a critical gradient model [18,19,20]. In these works, the turbulent diffusivity was written under the form

$$\chi_T = \Lambda q^{\nu} T^{3/2} \left(\frac{-\partial_r T}{T} - K \right)^{\eta} H \left(\frac{-\partial_r T}{T} - K \right) \tag{24}$$

Models (1) and (24) are equivalent when $\eta = 1$, which turns out to be consistent with experimental results. Comparing these models yield the relations $\kappa_c = RK$ and $\chi_s = 0.22M^{-0.5}B_T^2\Lambda$. The aim of this section is not to fully assess the transport model Eq.(1) with respect to experiment but rather to compare the values of χ_0, χ_s, and κ_c deduced from existing experiments to those deduced from a two term scaling law.

Pulse No:	$\chi_{0,e}$	$\chi_{s,e}$	$\kappa_{c,e}$	$\lambda_{0,e}$
JET 55809	0.7	4	5	0.035
JET 55804	1.2	1.5	5	0.160
JET 58148	0.8	3	5	0.053
JET 53822	0.5	1.5	4.8	0.069
JET 55805	0.5	6	5	0.017
AUG 14793,94	0.01	0.25	3	0.013
AUG 13556,58	0.1	0.15	5	0.133
AUG 17788,89	0.01	0.13	8	0.010
AUG 10591	0.85	0.99	6	0.143
AUG 12935	0.28	0.14	4	0.5
AUG 7806	1.79	1.4	7	0.183
AUG 17175	0.32	3	7	0.015
FTU	0.7	0.5	7.5	0.187

Table I: Values of $\chi_{s,e}$, $\chi_{0,e}$, $\kappa_{c,e}$ and $\lambda_{0,e}$ in JET, ASDEX-Upgrade, and FTU. All pulses are in L-mode except JET Pulse No: 58148 (H-mode), and AUG 13556, 17789 (partly in Ohmic).

Electron stiffness is investigated first here, summarising the results of experiments in ASDEX-Upgrade, JET and FTU. In ASDEX-Upgrade (R = 1.65m, a = 0.5m), dedicated experiments were performed in L mode with ECRH modulation. The Electron Cyclotron Resonant Heating (ECRH) power was deposited at two radial positions in such a way that the total power was constant. This procedure allowed varying $\nabla T_e/T_e$ over a large range of values while maintaining a constant edge temperature T_a. The modulated profiles were modelled with the model Eq.(24) and led to values of $\chi_{0,e}$, $\chi_{s,e}$, and $\kappa_{c,e}$ [19]. A similar analysis was done by F. Imbeaux et al. [18] with another set of experiments.

In JET (R=3m, a=1m), experiments using modulated Ion Cyclotron Resonance Frequency (ICRF) heating with a steady background of Neutral Beam Injection (NBI) heating have been done in L-mode [20] and H-mode [27]. A mode conversion scheme was used with 18% of He^3 in D plasmas

(P_{ICRF}=3.7MW). Electrons are directly heated when using this Ion Cyclotron Heating scheme, with good localisation properties. The position of the mode conversion layer was changed and the NBI power was varied from 2 to 9MW in order to cover a large range of temperature gradients. The 3 parameters $\chi_{0,e}$, $\chi_{s,e}$, and $\kappa_{c,e}$ were found by fitting both the steady and modulated profiles [20]. In FTU (R=0.96m, a=0.28m), a series of 9 ECRH heated plasmas was used. The power was not modulated in these experiments, but the heating location was changed. A least square minimisation technique provided the parameters $\chi_{0,e}$, $\chi_{s,e}$, and $\kappa_{c,e}$.

All these plasmas have been analysed with the same model Eq.(24) with $\nu = 3/2$. The principal difficulty is the determination of the background diffusivity $\chi_{0,e}$, given the experimental uncertainties (one reason could be the ad-hoc choice of an electrostatic gyroBohm scaling for the background diffusivity). The result of this multi-machine comparison is shown in Table I.

The thresholds in table I range between 3 and 7.5, which are typical values expected for ITG/TEM modes. The range of variation of the stiffness parameter $\chi_{s,e}$ is found to be wider. It lies between 0.25 and 2 when $T_e/T_i>1$. Larger values ($\chi_{s,e}$,~3÷6) are obtained in JET with dominant ion heating, when $T_e\approx T_i$. This finding is consistent with a recent study by Asp et al. investigating the effect of the ratio T_e/T_i on confinement using the Weiland model [28]. In this work, both electron and ion diffusivities are found to increase with T_e/T_i when heating electrons at fixed ion temperature. However diffusivities are also observed to increase when T_e/T_i goes down by heating ions at fixed Te. The latter result agrees with the trend that is observed here since the points at $T_e = T_i$ in Fig.7 correspond to larger ion heating with about the same electron heating as compared to the other points for which $T_e>T_i$. However the effect that is found experimentally is larger than the one found when using the Weiland model [27]. Finally we note that an opposite behaviour was found for χ_e in DIII-D in steady-state experiments, i.e. a degradation of the confinement when increasing T_e/T_i, although the latter result was obtained in a different range of parameters, namely $T_e/T_i<1$ [29].

Ion stiffness is less documented than electron stiffness because the ion temperature is difficult to measure in modulation experiments with the appropriate time resolution. This question has nevertheless been investigated in DIII-D, JET and ASDEX-Upgrade by analysing the steady ion temperature profiles in various regimes [5,6,30]. It was found in JET and ASDEX-Upgrade that $\kappa_{c,i}$ ranges between 5 and 8. The scatter is reduced when accounting for the dependence on T_e/T_i and the E×B velocity shear. For $T_e = T_i$ and low shear rate, the value of the threshold is $\kappa_{c,i} = 5.3$, which is close to the value found for electrons in JET. The stiffness factor was not obtained in this case since its value is difficult to obtain with steady-state profiles. In fact, the values of the threshold were obtained by assuming that the profiles are stiff enough to be close to the marginal profiles between $\rho = 0.2$ and $\rho = 0.6$. Modulation experiments done at JET are currently under analysis to clarify this issue.

5.2 CONDITIONS FOR STIFFNESS

The transport model Eq.(1) can be tested in several ways. One is a direct inspection of the temperature profiles. A set of electron temperature profiles coming from ASDEX-Upgrade is shown

10

in Fig.8 in Ohmic and ECH L-mode plasmas at $I_p = 400kA$ and $I_p = 1MA$ [19]. Profiles obtained in JET plasmas when combining mode conversion ICRF and NBI heating are shown on Fig.9 [20]. The scaling temperature T_{gB} is indicated on each profile. A change of slope occurs in general when $T_e \approx T_{gB}$, except for plasmas in ASDEX-Upgrade at $I_p = 1MA$, where Eq.(8) predicts a value of T_{gB} that is too large. Interestingly, using a value of T_{gB} calculated with the values of χ_s and κ_c deduced from the two term scaling law (see next section, Eq.(29)) is in better agreement with experiment. We note also that the change of slope is sharper than expected (the transition at $T_e \approx T_{gB}$ is a smooth one). At this point, it is stressed that other reasons may explain a different behaviour in the edge: for instance a change of the underlying instability, the influence of the Scrape-Off Layer, or an effect of collisionality. Another interesting feature is the change of gradients that occurs in JET core plasmas. No sawtooth is observed in the plasmas shown in Fig.9. So this change of slope may correspond to the transition between stiff and core regions that is expected when the gradient length crosses the stability threshold. Note that the ASDEX-Upgrade plasmas at $I_p = 1MA$ shown on Fig.8 (right panel) exhibit sawteeth, which flatten the temperature profile. Thus the change of slope at $\rho = 0.45$ likely corresponds to the $q = 1$ magnetic surface, masking a possible transition from stiff to non stiff regions. The transition from the stiff region to the edge region is believed to be at $\rho \approx 0.8$ for the Ohmic case and at $r^a 0.9$ for the case $P_{ECRH} = 1.6MW$. This is in agreement with the model prediction that the stiff region extends further out with increasing temperature.

   Another analysis consists in drawing $-\nabla T_e / T_e$ versus T_e / T_{gB}. For a stiff profile, this curve is expected to be universal at a given value of $\lambda_{0,e}$, as shown by Eq.(10). The exercise has been done in ASDEX-Upgrade (Fig.10) and in JET (Fig.11). These figures exhibit some similarity with Fig.1. The main features predicted by the model Eq.(1) are recovered. In particular, the region where the gradient length is close to the threshold is wider when the heat deposition profile is more localised in the core. This trend is observed when comparing ECRH with Ohmic heating (Fig.10), or when comparing off-axis with on-axis heating in JET plasmas (see Fig.11).

5.3 COMPARISON WITH A TWO TERM SCALING LAW.

The ITPA group has proposed two scaling laws for the global confinement time of the plasma bulk [8]. They correspond to two different hypotheses for the physics underlying the confinement in the pedestal region. The first one assumes that the edge confinement is controlled by thermal conduction with some degradation with β, while the second relies on an MHD β limit within the pedestal region. In terms of accuracy, these two models are equivalent. We will analyse in detail the model with MHD limited edge, because it corresponds to a confinement in the bulk that is gyroBohm and electrostatic, i.e. consistent with the assumptions underlying the model used here. More precisely the scaling law for the bulk region is

$$\tau_{ITPA,bulk} = 0.15 M^{0.34} \kappa^{-0.34} \varepsilon_a^{1.96} R^{2.32} I_{p,MA}^{0.68} B_T^{0.13} n_{a,19}^{0.59} P_{MW}^{-0.58} \qquad (25)$$

The normalised confinement time $B\tau_E$ scales as $\rho^{*-3}\beta^{0.05}$, which is close to an electrostatic gyroBohm scaling law. Using the relation

$$q = \frac{1+\kappa^2}{2}\frac{a^2 B_T}{R I_{p,MA}}$$ (26)

 one finds

$$\tau_{ITPA,bulk} = 0.45 M^{0.34}\kappa^{-0.34}\left\{\frac{1+\kappa^2}{2}\right\}^{0.68}\varepsilon_a^{3.32}R^3 q_a^{-0.68}B_T^{0.81}n_{a,19}^{0.59}P_{MW}^{-0.58}$$ (27)

to be compared with the Eq.(19) when using the expression of τ_{gB} given by Eq.(A11)

$$\tau_{ITPA,bulk} = 0.179 C_{ITPA}\chi_{s,eff}\kappa_c^{-4/5}M^{-1/5}\kappa^{7/5}\left\{\frac{1+\kappa^2}{2}\right\}^{-2/5}\varepsilon_a^{8/5}R^3 q_a^{-2v/5}B_T^{4/5}n_{a,19}^{3/5}P_{MW}^{-3/5}$$ (28)

The exponents of power, density, magnetic field, safety factor and major radius are similar in Eqs(27) and (28). Note that the agreement for the safety factor comes from the choice $v = 3/2$. This choice is however quite arbitrary, and would deserve a better assessment using both theory and experiments. Some significant differences between Eqs(27) and (28) appear in the exponent of the inverse aspect ratio $\varepsilon_a = a/R$, elongation, and mass, thus suggesting a dependence of the stiffness parameter on geometry factors. Assuming a "typical" case $\kappa = 1.6$, $\varepsilon_a = 1/3$, and $M = 2$, it is found that Eq.(27) matches Eq.(28) if $\chi_{s,eff}^{2/5}\kappa_c^{4/5} = 2.20 C_{ITPA}$. The contour lines of C_{ITPA} are shown in Fig.12 for a large domain of variation of the parameters λ_0 and T_a/T_{gB}. It is found that C_{ITPA} remains in the interval $1\div3$. Choosing $\kappa_c \approx 5$, one finds that $\chi_{s,eff}$ should be in the range $0.3\div4.5$. This is a large interval, which has to be reduced by transport analysis of steady-state and transient regimes. Choosing a medium value $C_{ITPA} = 2.0$ and $\kappa_c \approx 5$ yields a stiffness factor $\chi_{s,eff} \approx 1.6$. It is reminded here that $\chi_{s,eff}$ is an effective stiffness factor. For equal temperatures, $\chi_{cs,eff}$ is the sum of electron and ion stiffness parameters, $\chi_{s,eff} = \chi_{s,e} + \chi_{s,i}$. Thus $\chi_{s,e}$ and $\chi_{s,i}$ should be of order unity. The choice $\chi_{s,eff} \approx 1.6$ leads to the following "practical" expressions of the scaling temperature T_{gB} and the confinement time of the plasma bulk.

$$T_{gB,keV} \approx 0.43\left\{\frac{1+\kappa^2}{2\kappa}\right\}^{-2/5}M^{-1/5}\varepsilon_a^{-2/5}q_a^{-3/5}B_T^{4/5}n_{a,19}^{-2/5}P_{MW}^{2/5}$$ (29)

and

$$\tau_{Ebulk} \approx 0.081 M^{-1/5}\kappa^{7/5}\left\{\frac{1+\kappa^2}{2}\right\}^{-2/5}\varepsilon_a^{8/5}R^3 q_a^{-3/5}B_T^{4/5}n_{a,19}^{3/5}P_{MW}^{-3/5}$$ (30)

The ITPA database has been used to compare the pedestal height T_a to T_{gB}, given by the expression (29). The result is shown in Fig.13. It is found that T_a ranges between $0.5T_{gB}$ and $2T_{gB}$. However this result must be considered with caution since the stiffness factor could depart significantly from

the value $\chi_{s,eff} \approx 1.6$ chosen here. The trend is that the ratio T_a/T_{gB} is greater in large devices JT-60U and JET than in the medium size devices DIII-D and ASDEX-Upgrade. This is an interesting feature in view of Fig.3. Indeed, the stiff region was found to reach its maximum size for $T_a \approx T_{gB}$ and decreases when T_a/T_{gB} increases. This may explain why large devices are claimed to be "less stiff" (or not stiff at all). In spite of a higher pedestal that makes the edge stiffer, the width of the core region, which is sub-critical, could be larger in those plasmas, in particular in the H mode.

A pending question is the compatibility of the two term scaling law with the values of stiffness factor deduced from modulation experiments (table I). This is a delicate point since most of these plasmas are in L-mode, with ratios T_e/T_i different from 1, whereas the ITPA database deals with H-mode plasmas, with $T_e \approx T_i$. It is expected that the core physics is the same in L and H-mode. Similar values of $\lambda_{s,e}$ were found in L-mode (Pulse No: 55809) and H-mode (Pulse No: 58148) plasmas on JET, thus providing some support to this assumption. The range of stiffness factor $\chi_{s,eff}$ that is compatible with the global scaling law is 0.3÷4.5. It is reminded here that $\chi_{s,eff} = (T_e/T_i)^{5/2} \chi_{s,e} + \chi_{s,i}$. Regarding the values of stiffness factor obtained from heat wave analysis, while there is no problem of compatibility with the values $\chi_{s,e} \sim 0.25 \div 2$ found in conditions $T_e > T_i$, the high values $\chi_{s,e} = 3 \div 6$ at $T_e \sim T_i$ appear too large by a factor 1.5÷2.5 assuming $\chi_{s,e} = \chi_{s,i}$. A sensitivity study indicates that the heat wave analysis becomes less sensitive to the value of $\chi_{s,e}$ at high $\chi_{s,e}$ values. Moreover it can be noted that a significant scatter of points is present in Fig.7, which is mainly due to the fact that the simple model assumed does not always allow a perfect reproduction of the data, and some trade off in the fit of the various quantities often needs to be accepted. Taking also into account the various simplifications introduced into this analysis, we consider that these results are encouraging. Clearly some further measurements will be necessary to reduce this uncertainty. The observations suggest that the ratio T_e/T_i plays an important role, which will have also to be investigated further in detail in the future.

Finally it is interesting to compare the present range of stiffness factors with theoretical expectations. The IFS-PPPL model [11] is close to the form Eq.(1) when simplified, i.e. , choosing $Z_{eff} = 1$, $r/R \ll 1$, $R/L_n = 0$,

$$\chi_{Ti} = \frac{12}{1 + s^{0.84}} \left(q \frac{T_e}{T_i} \right)^{1.1} \frac{c_s \rho_s^2}{R} \left(\frac{-R \partial_r T}{T} - \kappa_C \right) H \left(\frac{-R \partial_r T}{T} - \kappa_C \right)$$

We note that the exponent of q is $\nu = 1.1$. Choosing $T_i = T_e$, and a magnetic shear $s = 1$, one gets $\chi_{si} \approx 6$. An estimate of χ_{se} is harder to provide, since it depends on collisionality.

The GLF23 model [12] is a more sophisticated model, which uses a calculation of growth rates. So it cannot be easily reduced to an expression of the form Eq.(1). However it was mentioned in the original paper that the stiffness factor is similar to the IFS-PPPL model. A renormalized model was proposed recently [31], where the stiffness factor of ITG/TEM driven transport was reduced by a factor 3.7. Using the IFS-PPPL value, this leads to an estimate $\chi_{si} \approx 1.6$. The Weiland model is also based on a comprehensive calculation of growth rates. Numerical scans indicate that $\chi_{si} \approx 1$ and

$\chi_{se} \approx 0.3$. Finally several theoretical models and turbulence simulations were compared in the CYCLONE group [21]. The results from the LLNL gyrokinetic code were fitted by the expression

$$\chi_{Ti} = 5 \, \frac{c_s \rho_s^2}{R} \left(\frac{-R\partial_r T}{T} - \kappa_C \right) H \left(\frac{-R\partial_r T}{T} - \kappa_C \right)$$

where $\kappa_c = 6$. The simulations were done at fixed ratio of density to temperature gradient length $L_n/L_T = 3.1$, with $Z_{eff} = 1$. We note that there is no q dependence in this expression, i.e. $\chi_{si} = 5/q^\nu$. Since the simulations were done at $q = 1.4$, one gets an estimate $\chi_{si} \approx 3$. In summary, it is found that c_{si} ranges between 1 and 6 depending on the model. The electron stiffness factor is less documented. It is typically 3 times smaller that the ion stiffness. We stress here that these values are purely indicative, as these models exhibit rather complex parametric dependences. Nevertheless we can conclude that the range of variation of the stiffness factor found in the literature is quite large, and compatible with both our experimental results and the value deduced from the ITPA scaling law.

SUMMARY

Using the critical gradient transport model

$$\chi_T = \chi_s \, q^\nu \, \frac{T}{eB} \, \frac{\rho_s}{R} \left(\frac{-R\partial_r T}{T} - \kappa_C \right) H \left(\frac{-R\partial_r T}{T} - \kappa_C \right) + \chi_0 q^\nu \, \frac{T}{eB} \, \frac{\rho_s}{R}$$

it is found that:

1) Choosing an exponent $\nu = 3/2$, the proximity of a profile to a marginally stable state (stiffness) is then characterised by 3 numbers: the degree of stiffness $\lambda_0 = \chi_0/\kappa_c\chi_s$, the ratio T_a/T_{gB}, and the width of the deposition profile. Here T_a is the edge temperature and the reference temperature T_{gB} satisfies the condition

$$\Gamma_T(a) = \chi_s \, \kappa_c^2 q_a^\nu \, n_a \, T_{gB} \, \frac{T_{gB}}{eB} \, \frac{\rho_{s0}}{R}$$

where $\Gamma_T(a)$ is the thermal flux at the edge. Profiles get stiffer when λ_0 decreases, T_a/T_{gB} increases or when the heating source is more central.

2) The confinement time of the plasma bulk (without the pedestal contribution and for an elliptical geometry) is

$$T_{EBulk} = 0179 C_{ITPA} \, \chi_{s,eff}^{-2/5} \kappa_c^{-4/5} M^{-1/5} \kappa^{7/5} \left(\frac{1+\kappa^2}{2\kappa} \right)^{-2/5} \varepsilon_a^{8/5} R^3 B_T^{4/5} q_a^{-3/5} n_{a,19}^{3/5} P_{MW}^{-3/5}$$

In this formula, the stiffness factor $\chi_{s,eff}$ is an effective value $\chi_{s,eff} = \chi_{s,e} + \chi_{s,i}$, where $\chi_{s,e}$ and $\chi_{s,i}$ are the electron and ion stiffness factors (the threshold κ_c and the degree of stiffness λ_0 are supposed to be the same for electrons and ions). The form factor C_{ITPA} depends on the normalised edge

14

temperature T_a/T_{gB} and the degree of stiffness λ_0. It decreases with the normalised edge temperature for non stiff profiles. On the contrary it increases linearly with the edge temperature for stiff profiles. In the general case, C_{ITPA} is a sum of the contributions of stiff and non stiff regions, which behave in opposite ways. The two term scaling law proposed by the ITPA-CDBM group corresponds to intermediate values of λ_0, typically in between 0.01 and 0.1, which indeed is approximately the range of values observed in the heat modulation experiments for electrons (table I). Choosing this range of stiffness factors and varying the edge temperature in a wide domain, it is found that $1 < C_{ITPA} < 3$.

3)   This model has been applied for electrons at JET, ASDEX-Upgrade and FTU (mainly modulation experiments in the electron channel). The stiffness parameter χ_{se} was found to cover a wide range of variation, i.e. ranges between 0.25 and 6. A correlation has been found between the stiffness χ_{se} and the ratio T_e/T_i in these plasmas: χ_{se} decreases with increasing values of T_e/T_i.

4) A comparison between this transport model and the ITPA two term scaling law leads to the relation $\chi_{s,eff}^{2/5} \kappa_c^{4/5} = 2.2 C_{ITPA}$. Choosing C_{ITPA} in the range $1 \div 3$ and $\kappa_c \approx 5$, one finds that $\chi_{s,eff}$ should be in the range $0.3 \div 4.5$. The medium value $C_{ITPA} = 2.0$ yields a stiffness parameter $\chi_{s,eff} \approx 1.6$, i.e. a value of the order of unity for each species. The range $0.3 \div 4.5$ is compatible with the results found in JET, ASDEX-Upgrade and FTU given the simplicity of the model that is used. Still it should be possible to refine this range in the future.

CONCLUSION

A critical gradient transport model that covers the basic properties of turbulent transport has been used extensively. This model contains only 3 free parameters that can be deduced from actual experiments in tokamaks. It also provides a quantitative criterion to get stiff profiles, thus providing a way to assess quantitatively this controversial issue. It is found that increasing the edge temperature does not necessarily lead to an overall stiffer profile. Indeed there exists usually a region in the core where the temperature gradient is below the stability threshold, and is therefore not stiff. This core region broadens when the edge temperature increases. This property explains why a transport model with a threshold can still be compatible with the two term scaling law developed by the ITPA-CDBM group. This model has been applied to analyse a variety of experiments using mostly electron heat modulation on JET, ASDEX-Upgrade and FTU. The thresholds are found to be in the expected domain for ITG/TEM modes. The stiffness factor deduced from modulation experiments is found to increase when decreasing T_e/T_i. The latter observation suggests that the ratio T_e/T_i plays an important role in confinement. The values of the stiffness factor are compatible with the expectation from theory. The range of variation deduced from modulation experiment is larger than the one estimated from the ITPA-CDBM two term scaling law. This difference appears to be compatible

with the simplifications underlying this transport model, and also with the various uncertainties when determining the models parameters from modulation experiments and global scaling laws.

Thus these results can be considered as encouraging. Still further experiments are needed to better determine the parametric dependences of the threshold and more importantly of the stiffness factor. The present study suggests a dependence on the ratio of T_e/T_i. This raises the question of the coupling between electron and ion channels, or in terms of stability between ITG and TEM branches. This coupling may lead to a dependence of the heat flux of one species on the temperature gradient length of another species, in addition to the temperature itself. The clarification of this point will require a large number of experiments in a variety of electron and ion heating scenarios. Also the value of the stiffness factor depends sensitively on the choice of scaling that is done with respect to the safety factor and geometrical factors. The latter point is illustrated by the difference between the two term global scaling law and the present model in terms of shaping and aspect ratio parameters. Regarding this question, changing the profile of safety factor would be useful, for instance by generating a non-inductive part of the current. The last issue is the comparison of a critical gradient model with global scaling laws. The nature and scaling of the background diffusivity plays an important role, because it determines the width of the non stiff core region. Reducing the uncertainty on this parameter would allow a more reliable comparison. Also the present model should be used more extensively in H-mode plasmas, to be compared directly with the ITPA database.

APPENDIX A

NORMALISATION OF THE HEAT EQUATION

The heat flux is linked to the gradient via the Fourier law

$$\Gamma_T = -n\chi_T \partial_r T \tag{A1}$$

It is also the radial integral of the heat source Pheat

$$\Gamma_T = \frac{1}{</\nabla r/^2>V'} \int_0^r dr V' P_{heat}(r) \tag{A2}$$

where

$$V' = 2\pi\psi' \int_0^{2\pi} \frac{d\theta}{B.\nabla\theta} \tag{A3}$$

We now solve the heat equation Eq.(A2) with the transport model Eq.(1). It is convenient to introduce a normalised spatial coordinate

$$\rho = \frac{5}{2} \kappa_c \frac{a-r}{R} \tag{A4}$$

(the magnetic axis is located at $\rho = \rho_{max} = 5\kappa_c a/2R$ and the edge at $\rho = 0$, also $\rho/\rho_{max} = 1-r/a$). The parameter

$$\lambda_0 = \frac{\chi_0}{\kappa_c\chi_s} \tag{A5}$$

characterises the relative degree of stiffness and is supposed to be smaller than 1. Finally we define a normalised temperature

$$\tau = \left\{\frac{T}{T_{gB}}\right\}^{5/2} \tag{A6}$$

and a normalised heat flux $g(\rho) = G(r)/G(a)$ with

$$G(r) = \frac{1}{n(r)[q(r)]^\nu</\nabla r/^2>V'(r)} \int_0^r dr V' (r) P_{heat}(r) \tag{A7}$$

The relation

$$\Gamma_T(a) = \chi_s\kappa_c^2 q_a^\nu n_a T_{gB} \frac{T_{gB}}{eB} \frac{\rho_{s,gB}}{R^2} \tag{A8}$$

defines the temperature T_{gB}. The flux $\Gamma_T(a)$ is equal to the heating power P divided by a surface

$S = C_s 2\pi R 2\pi a$, q_a the edge safety factor and n_a the edge density. The shape factor C_s is defined as

$$C_s = \frac{<|\nabla r|^2>_{r=a} V'_a}{2\pi R 2\pi a} \tag{A9}$$

For an elliptical geometry, $<|\nabla r|^2> = (1 + \kappa^2)/2\kappa^2$, $V' = 2\pi R 2\pi\kappa r$ and $C_s = (1 + \kappa^2)/2\kappa$, where κ is the elongation.

The temperature T_{gB} exhibits the usual "gyroBohm" scaling. It will play an important role in this calculation. It may be recast in a more convenient way when the geometry is elliptical

$$T_{gB,keV} = 1.89 \left\{ \frac{1 + \kappa^2}{2\kappa} \right\}^{-2/5} \chi_s^{-2/5} \kappa_c^{-4/5} M^{-1/5} \varepsilon_a^{-2/5} q_a^{-2\nu/5} B_T^{4/5} n_{a,19}^{-2/5} P_{MW}^{2/5} \tag{A10}$$

We also define a reference "gyroBohm confinement time" τ_{gB}

$$T_{gB}(s) = \frac{3 n_a T_{gB} V}{P} = 0.179 C_{sh} \chi_s^{-2/5} \kappa_c^{-4/5} M^{-1/5} R^3 \varepsilon_a^{8/5} q_a^{-2\nu/5} B_T^{4/5} n_{a,19}^{3/5} P_{MW}^{-3/5} \tag{A11}$$

The shaping factor C_{sh} is $C_{sh} = C_v C_s^{-2/5}$ where the volume form factor C_v is such that $V = C_v 2\pi R \pi a^2$. In elliptical geometry $C_s = (1 + \kappa^2)/2\kappa$ and $C_v = \kappa$, so that $C_{sh} = \kappa^{7/5}((1 + \kappa^2)/2)^{-2/5}$. The units are lengths in meters, B_T in Teslas, the density in 10^{19} m^{-3} and the power in MW. $\varepsilon_a = a/R$ is the inverse aspect ratio. As an illustration, the values $\kappa_c = 5$ and $\varepsilon_a = 1/3$, (i.e. $r_{max} = 5$) will be chosen in the following. Typical values are $\chi_0 \approx 0.1$, $\chi_s \approx 1$, and $\kappa_c = 4 \div 6$. The normalised ratio $\lambda_0 = \chi_0/\kappa_c\chi_s$ is therefore a small number. The value $\lambda_0 = 0.025$ is chosen as an example in this paper. With the normalisation above, the heat law becomes particularly simple ($\tau' = \partial\rho\tau$)

$$\tau \left\{ \frac{\tau'}{\tau} - 1 \right\} H \left\{ \frac{\tau'}{\tau} - 1 \right\} + \lambda_0 \tau' = g \tag{A12}$$

APPENDIX B

ANALYTIC SOLUTION FOR CONSTANT OR EXPONENTIAL FLUX

If the heat flux $\gamma(\rho)$ is a constant (=1), the solution of Eqs.(11) is analytic, i.e. using the change of variable $\cosh(u) = (1 - \lambda_0)^2 \frac{\tau}{2} + 1$:

Above the threshold, $0 < \rho < \rho_{cr}$, $\tau_a < \tau < 1/\lambda_0$

$$\rho = F(\tau) - F(\tau_a)$$

$$F(\tau) = \frac{1}{(1-\lambda_0)} \, \mathrm{Log}\left\{ 1 + (1-\lambda_0)^2 \, \frac{\tau}{2} + (1-\lambda_0)\left[(1-\lambda_0)^2 \, \frac{\tau^2}{4} + \tau \right]^{1/2} \right\}$$

$$+ \left[(1-\lambda_0)^2 \, \frac{\tau^2}{4} + \tau \right]^{1/2} - (1-\lambda_0) \, \frac{\tau}{2} \tag{B1}$$

$$\rho_{cr} = -\frac{1}{(1-\lambda_0)} \, \mathrm{Log}(\lambda_0) + 1 - F(\tau_a) \tag{B2}$$

$$\rho_{gB} = F(1) - F(\tau_a) \tag{B3}$$

Approximate expressions of the function F are the following

$$\tau \gg 1, \;\; F(\tau) \approx \mathrm{Log}(\tau)/(1-\lambda_0) \;\; ; \quad \tau \ll 1, \;\; F(\tau) \approx 2\tau^{1/2}$$

Below the threshold, $\rho > \rho_{cr}, \tau > 1/\lambda_0$

$$\tau = \frac{1 + \rho - \rho_{cr}}{\lambda_0} \tag{B4}$$

If the heat source is exponential $g(\rho) = \exp((1-\lambda_0)\rho)$, one may make the change of function

$$\tau = \theta e^{(1-\lambda_0)\rho} \; ; \tau_a = \theta_a \tag{B5}$$

Above the threshold, the function θ is then solution of the equation

$$\theta'^2 + \theta(1-\lambda_0)\theta' - g\theta = 0 \tag{B6}$$

This equation is close to Eq.(12). Its solution is

$$\rho = G(\theta) - G(\theta_a) \tag{B7}$$

$$G(\theta) = F(\theta) + (1 - \lambda_0)\theta$$

The transition between the stiff and core region occurs when $\theta = 1/\lambda_0$, i.e. at the position

$$\rho_{cr} = - \frac{1}{(1-\lambda_0)} \, \mathrm{Log}(\lambda_0) + \frac{1}{\lambda_0} - G(\theta_a) \tag{B8}$$

Note that this value is much larger than in the constant g case. This confirms that a more peaked heating source induces a stiffer profile. The solution in the core region is

$$\tau = \frac{1}{1-\lambda_0} \left\{ \frac{1}{\lambda_0} \, g(p) - g(\rho_{cr}) \right\} \tag{B9}$$

APPENDIX C

ASYMPTOTIC EXPRESSIONS OF THE EDGE, CORE AND STIFF REGION CONTRIBUTIONS TO THE CONFINEMENT.

Edge region

The edge contribution, which corresponds to $\tau_a < \tau < 1$, can be approximated by the expression (assuming a small radial extend in the edge so that $g \approx 1$ and $J \approx 2$)

$$C_{\tau edge} = \frac{1}{\rho_{max}} \int_{\tau a}^{1} d\tau \tau^{-1/10} = \frac{10}{9\rho_{max}} \left\{ 1 - \tau_a^{9/10} \right\} \tag{C1}$$

The expression (C1) can be recast as

$$C_{ITPA,edge} \approx \frac{10}{9\rho_{max}} \left\{ 1 - \left\{ \frac{T_a}{T_{gB}} \right\}^{9/4} - \frac{9}{5} \frac{T_a}{T_{gB}} + \frac{9}{5} \left\{ \frac{T_a}{T_{gB}} \right\}^{1/2} \right\} \tag{C2}$$

It is interesting to note that this expression depends sensitively on the edge temperature The reason is that the transport model is a non linear function of the temperature, thus leading to some profile resilience, even if there is no threshold involved.

Core region

An approximate expression can be found assuming $g \approx a/r$,

$$C_{ITPA,edge} \approx \left\{ \frac{r_0}{a} \right\}^2 \int_0^{\infty} du e^{-u} \left\{ \left[\tau_0 + \frac{r_{max}}{2\lambda_0} u \right]^{2/5} - \tau_a^{2/5} \right\} \tag{C3}$$

When there exists a stiff region, one has $\tau_{cr} \approx a/(r_{cr}\lambda_0)$ and the pedestal contribution is negligible. The core contribution to the form factor is then an increasing function of the edge temperature.

Stiff region

In the general case, the profile is stiff within a layer. The contribution of a stiff layer $[\rho_{cr}, \rho_{gB}]$ (temperature $[\tau_{cr}, 1]$) is

$$C_{\tau stiff} = 2 \left\{ \frac{5}{2\rho_{max}} \right\}^2 \left\{ \left[\frac{2}{5} (\rho_{max} - \rho_{cr}) + 1 \right] \tau_a^{2/5} - \left[\frac{2}{5} (\rho_{max} - \rho_{gB}) + 1 \right] \right\} \tag{C4}$$

In presence of edge and core regions $\tau_{cr} = g_{cr}/\lambda_0$ where gcr is the normalised heat flux at the transition to the core region. Thus this contribution varies as the width $\rho_{cr} - \rho_{gB}$ of the stiff region. When the edge temperature increases, the edge non stiff region disappears and this width increases. It then shrinks because the core region broadens.

REFERENCES

[1]. B. Coppi and N. Sharky, Nucl. Fusion **21**, 1363 (1981).

[2]. F. Ryter, F. Leuterer, G. Pereverzev, et al., Phys. Rev. Lett. **86**, 2325 (2001).

[3]. G.T. Hoang, C. Bourdelle, X. Garbet, et al., Phys. Rev. Lett. **87**, 125001 (2001).

[4]. P. Mantica, et al., Plasma Physics and Controlled Fusion **44**, 2185 (2002)

[5]. D.R. Baker, et al., Phys. Plasmas **8**, 4128 (2001).

[6]. A.G. Peeters, Nucl. Fusion **42**,1376 (2002).

[7]. D.R. Mikkelsen, et al., Nucl. Fusion **43**, 30 (2003).

[8]. G. Cordey et al., Nucl. Fusion **43**, 670 (2003).

[9]. P.H. Rebut, P.P. Lallia, M.L. Watkins, in Plasma Physics and Controlled Nuclear Fusion Research 1988 (Proc. 12th Int. Conf. Nice, 1988), Vol.II, IAEA, Vienna (1989), 191.

[10]. H. Nordman, J. Weiland, A. Jarmen, Nucl. Fusion **30**, 983 (1990)

[11]. M. Kotschenreuther, W. Dorland, M.A. Beer, and G.W. Hammett, Phys. Plasmas **2**, 2381 (1995).

[12]. R.E. Waltz, G.M. Staebler, W. Dorland, et al., Phys. Plasmas**4**, 2482 (1997).

[13]. P. Zhu, G. Bateman, A.H. Kritz, W. Horton, Phys. Plasmas **7**, 2898 (2000).

[14]. M. Ottaviani, W. Horton, M. Erba, Plasma Phys. Cont. Fus. **39**, 1461 (1997).

[15]. M. Erba et al., Plasma Phys. Contr. Fusion **39**, 261 (1997).

[16]. V. Parail et al., Nucl. Fusion **37**, 481 (1997).

[17]. G. Tardini at al, Nucl. Fusion **42**, L11 (2002).

[18]. F. Imbeaux, F. Ryter and X. Garbet, Plasma Physics and Controlled Fusion **43**, 1503 (2001).

[19]. F. Ryter et al., Nucl. Fusion **43**, 1396 (2003).

[20]. P. Mantica, in proceedings of the 19th IAEA Fusion Energy Conference, Lyon 2002.

[21]. A.M. Dimits et al., Phys. Plasmas **7**, 969 (2000).

[22]. X. Garbet, R.E. Waltz, Phys. Plasmas **3**, 1898 (1996).

[23]. M. Ottaviani and G. Manfredi, Nucl. Fusion **41**, 637 (2001).

[24]. R. Waltz, J.M. Candy, M.N. Rosenbluth, Phys. Plasmas **9**, 1938 (2002).

[25]. Z. Lin, et al., 19th IAEA Fusion Energy Conference, Lyon 2002, submitted to Nucl. Fusion.

[26]. M. Ottaviani, Private comunication.

[27]. P. Mantica et al., in Proceedings of the 30th EPS conference on Controlled Fusion and Plasma Physics , St-Petersbourg, 2003.

[28]. E. Asp et al, to be submitted.

[29]. C.C. Petty et al., Phys. Rev. Letters **83**, 3661 (1999).

[30]. R. C. Wolf, Y. Baranov, X. Garbet, et al., Plasma Phys. Control. Fusion **45,** 1757 (2003)

[31]. J. Kinsey, et al, "Burning Plasma Confinement Projections and Renormalization of the GLF23 Driftwave Transport Model" to appear in Fusion Sci. Tech.
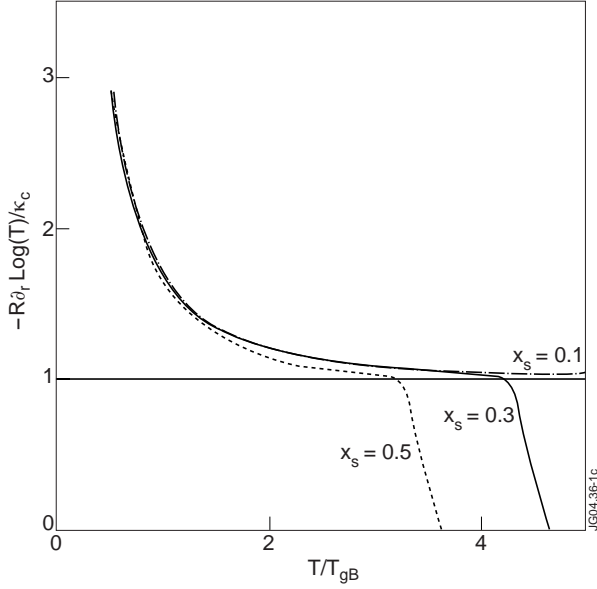
Figure 1: Logarithmic derivative of the temperature versus T/T_{gB} for $T_a/T_{gB} = 0.5$, $\lambda_0 = 0.025$ and 3 values of the heat deposition localisation ($x_s = 0.1$, 0.3, and 0.5). The horizontal line is the threshold.
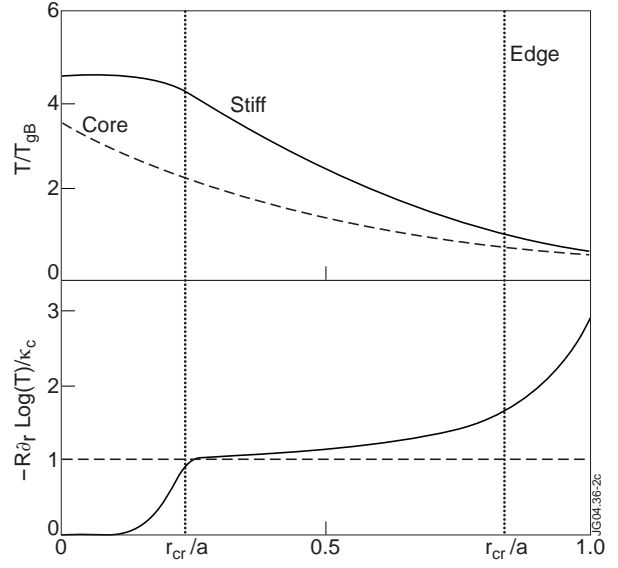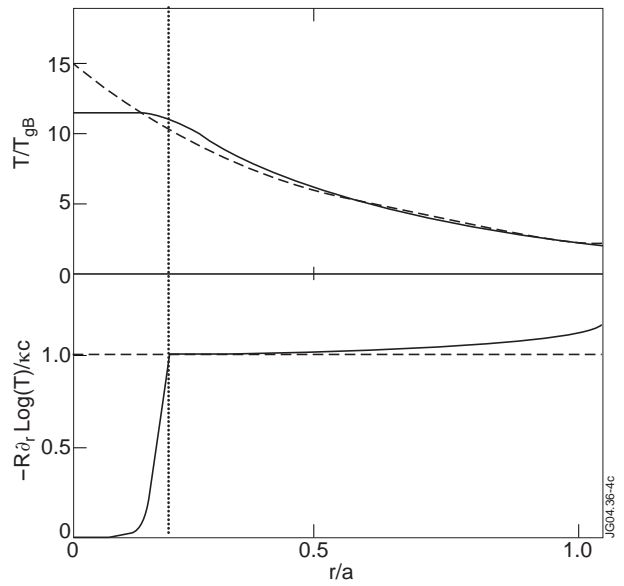

Figure 2: Profiles of the normalised temperature T/T_{gB} and its logarithmic derivative for $T_a/T_{gB} = 0.5$ and $\lambda_0 = 0.025$. The dashed lines correspond to a stiff profile $T = T_a e^\rho$ (and $-R\partial rT/T = \kappa_c$). The vertical dotted lines are the boundaries of the "non stiff" regions $\tau < 1$ (edge) and $\tau > g(\rho_{cr})/\lambda_0$ (core).
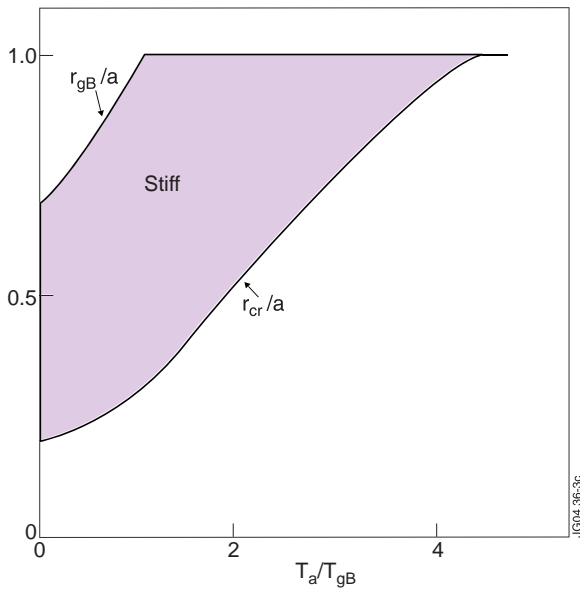
Figure 3: Stiffness layer (r_{cr}/a, r_{gB}/a) for $\lambda_0 = 0.025$ and increasing values of the edge temperature.

Figure 4: Profiles of the normalised temperature T/T_{gB} and its logarithmic derivative in a stiff case $T_a/T_{gB} = 2.0$ and $\lambda_0 = 0.001$. Same conventions as in figure 1.

23
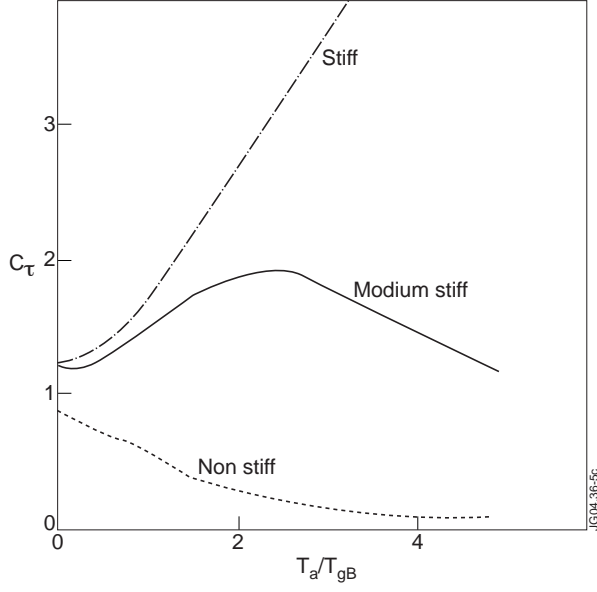
Figure 5: Form factor C_{ITPA} as function of the edge temperature for 3 cases: strongly stiff ($\lambda_0 = 0.001$), medium stiff ($\lambda_0 = 0.05$) and non stiff ($\lambda_0 = 0.9$) cases.
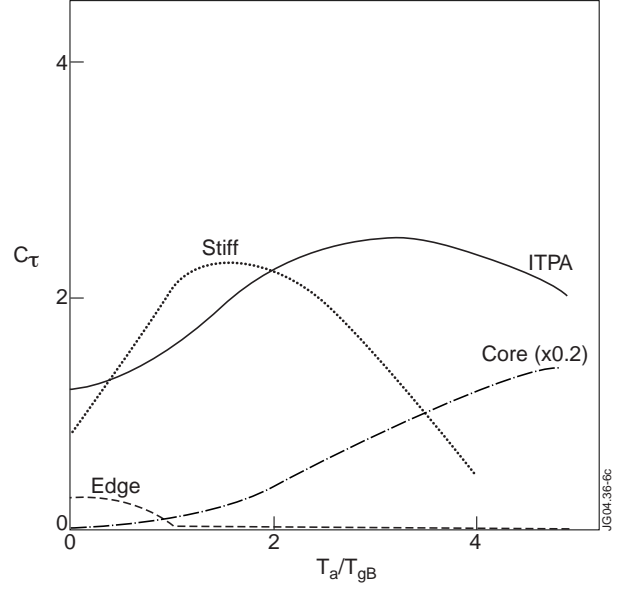
Figure 6: Variations of Ctedge, $C_{\tau stiff}$, $C_{\tau core}$, and $C_{\tau ITPA}$ as function of the normalised edge temperature for $\lambda_0 = 0.025$.
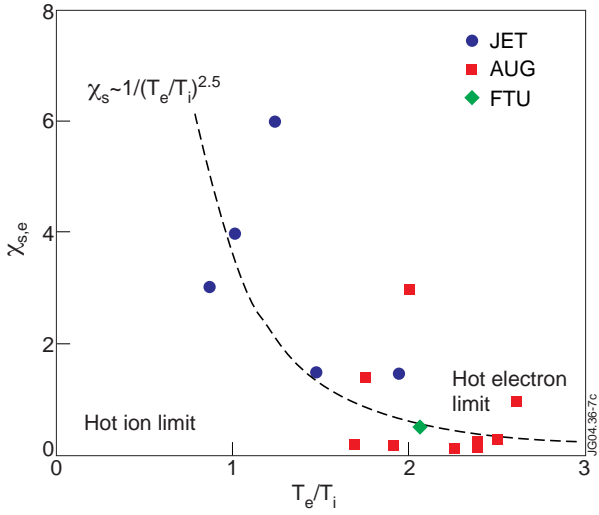

Figure 7: Electron stiffness $\chi_{s,e}$ versus ratio T_e/T_i deduced from modulation experiments in ASDEX-Upgrade and JET, and from a scan of the position of ECRH heating in FTU. The values of T_e and T_i are taken on the magnetic axis.
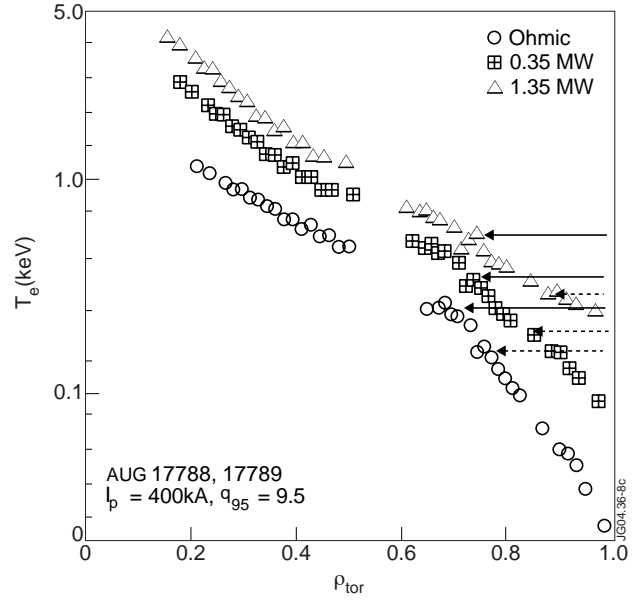
Figure 8: Comparison of T_{gB} with T_e profiles in ASDEX-Upgrade (L-mode) in Ohmic and ECRH heated plasma. Left panel: $I_p = 400kA$, $P_{ECRH} = 0$ (Ohmic), 0.35, and 1.35MW, no sawtooth. Right panel: $I_p = 1MA$, $P_{ECRH} = 0$ (Ohmic), 0.8, and 1.6MW, sawtoothing. Solid horizontal lines indicate T_{gB} given by Eq.(8), while horizontal dashed lines are the values of T_{gB} calculated with the values of stiffness parameter and threshold deduced from the ITPA two term scaling law Eq.(29).
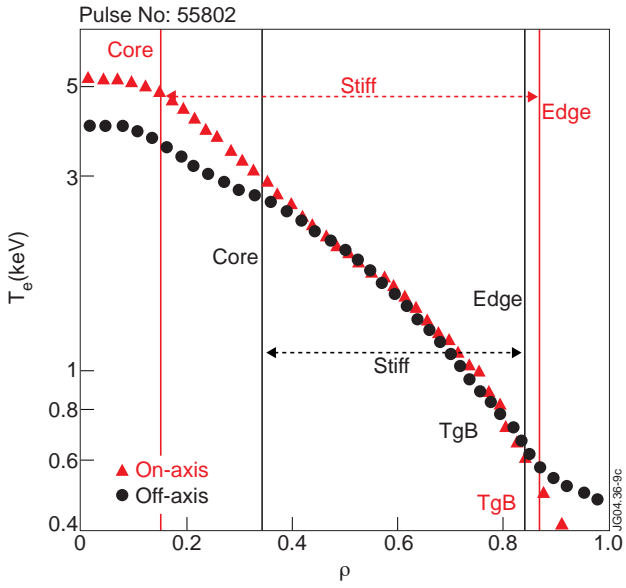
Figure 9: Experimental ECE T_e profiles for two JET discharges with on-axis and off-axis ICRH heating. Pulse No: 55802 (red):3.6MW ICRH on-axis, 3.2MW NBI; 55809 (black): 3.7MW ICRH off-axis, 9.1MW NBI. The reference temperature is indicated in the plot, the lines are the borders between edge, stiff and core regions (compare with Fig.8) .As expected, the pulse with on-axis heating has a wider stiff region
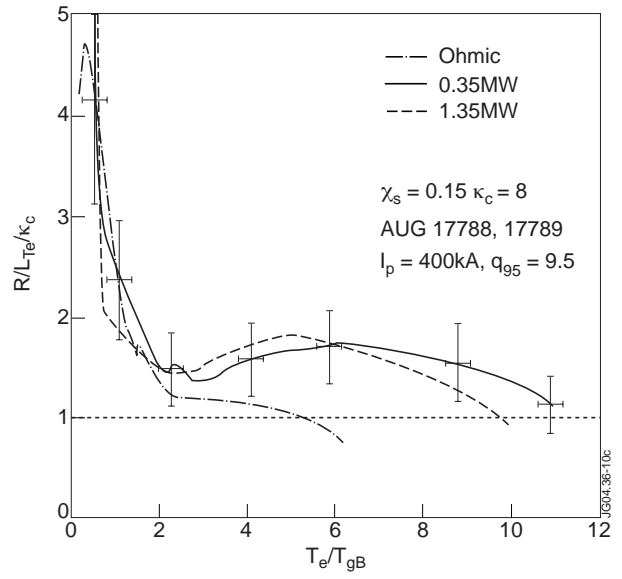

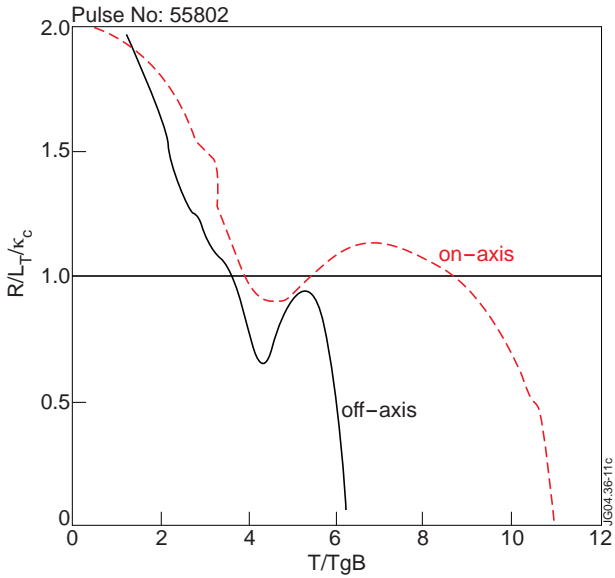*Figure 10: $-R\nabla T_e/T_e$ versus T_e/T_{gB} in ASDEX-Upgrade*

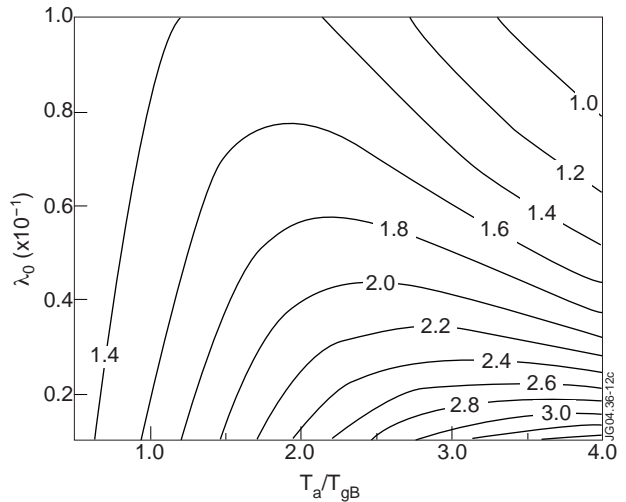*Figure 11: $-R\nabla T_e/T_e$ versus T_e/T_{gB} in JET.*

Figure 12: Contour lines of the form factor C_{ITPA} versus the normalised edge temperature and degree of stiffness l_0.

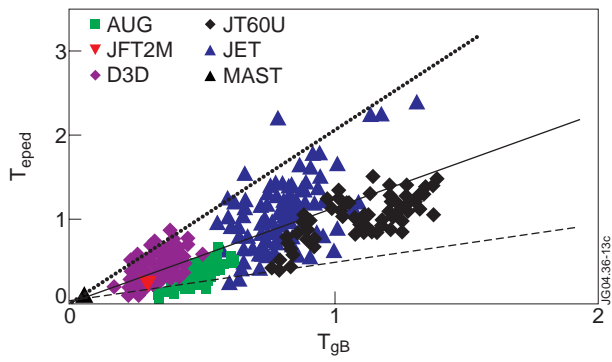*Figure 13: Pedestal temperature Ta versus the scaling temperature TgB. The lines indicate the identities $T_a=0.5T_{gB}$ (dashed), $T_a=T_{gB}$ (solid), and $T_a=2T_{gB}$ (dotted).*